실제적인 스윗치를 사용한 직류 변환기의 상태 공간 모델링 (II) : 모든 부수적인 요소 포함

임 춘택[0] , 정 규범 , 조 규형

한국 과학 기술원 전기 및 전자 공학과

PRACTICAL SWITCH BASED STATE-SPACE MODELING OF DC-DC CONVERTERS (PART II) : ALL PARASITICS

C. T. Rim , G. B. Joung and G. H. Cho

Dept. of Electrical Engineering, Korea Advanced Institute of Science and Technology

ABSTRACT

All parasitics such as switch conduction voltages, conduction resistances, switching times and ESR's of capacitors are counted in the new state-space modeling based on non-ideal switching functions. An equivalent simplified model is derived from the complex circuit with parasitics. Hence the results are very simple and exact, which are very important features of modelings. The pole frequency, dc voltage gain and efficiency of the general converter, the buck-boost converter are analyzed and verified by the experiments with good agreements with the theories. This may be a good summary for the previous works concerned with parasitics.

I. INTRODUCTION

In the modeling of switching systems, parasitics such as switch conduction voltages, conduction resistances, switching times and ESR's of capacitors are frequently ignored because of the difficulties in the modeling and the complexities in the result. This situation of excluding parasitics is very helpful for the understanding of the main features of a switching system. Most conventional modelings are thought to be adequate for this purpose. So it is no doubt that these modelings are successful in the primary stage of the design of a switching system. However the parasitic effects should be countered in the secondary stage of the design, where high performances such as high gain, efficiency and robustness of system poles are required. If we note the fact that the efficiencies of typical switching regulators are about 70-85 percents , the parasitics are frequently not negligible in practice. A few papers which deal with the effects in part are found, but a large part of them are based on computer simulations. These considerably reduce the effort in the modeling, however, they give solutions for only finite selected values with poor physical insight. Only a few papers are found which give analytical results useful for the secondary design. Parasitic resistances and part of switching times are counted in [1]. Rough description of all parasitics is found in [2]. And switching times are considered in [3]. Parasitics except the switching times are briefly explained in [4].

In this paper all parasitic effects are integrated into one as a summary of the previous works using a new state space modeling. The analytical results are quite simpler than the previous works but they are very exact. This feature of the modeling makes people understand the parasitics easily. It is identified that the conduction voltages can be dealt with separately from other parasitics in general. It is also verified that all parasitic resistances are integrated into an equivalent resistor.

The modeling procedure is shown for the buck-boost converter as the general converter among the buck, boost and buck-boost converters. The modeling is based on the state-space description and non-ideal switching functions. An equivalent circuit which eliminates all parasitics except switching times is derived without any approximation. This simplified circuit is found to be just the same circuit used in Part I [5]. Then the modeling is verified by the experiments with a good agreement with theories. The results are also summarized in a compact table.

II. MODELING PROCEDURE

It is assumed that the circuit elements are LTI and that the switches have finite switching times, conduction voltages V_Q and V_D and conduction resistances R_Q and R_D. The inductor and capacitor are assumed to have series resistances. Continuous conduction mode is assumed and the switching time modulation is permitted. The circuit to be modeled is shown in Fig. 1.

A. Equivalent State-Space Model

The derivatives of states of the buck-boost converter of Fig. 1a are found to be

$$L_o\dot{x}_1^* = s_1(t)\left[-x_2^*\frac{R_L}{R_C+R_L} - V_D\right] + s_3(t)\left[u^* - V_Q\right] - s_2(t)\,x_1^*\left[R_D + R_C /\!/ R_L\right] - s_4(t)\,x_1^*\,R_Q - R_{so}\,x_1^*$$

$$= -x_1^*\left[R_{so} + s_4(t)\,R_Q + s_2(t)\,(R_D + R_C /\!/ R_L)\right] - x_2^*\,s_1(t)\frac{R_L}{R_C+R_L} + u^*\,s_3(t) - s_3(t)\,V_Q - s_1(t)\,V_D \tag{1a}$$

$$C_o\dot{x}_2^* = s_2(t)\,x_1^*\frac{R_L}{R_C+R_L} - \frac{x_2^*}{R_C+R_L} \tag{1b}$$

and the output equation is represented as

$$y = s_2(t)\,x_1^*\,R_C /\!/ R_L + x_2^*\frac{R_L}{R_C+R_L} \tag{1c}$$

, where the switching functions $s_1(t)$ and $s_2(t)$ are the same as defined in Part I, and $s_3(t)$ and $s_4(t)$ are the complementary functions of $s_1(t)$ and $s_2(t)$, respectively, that is,

$$s_3(t) = 1 - s_1(t) \ , \quad s_4(t) = 1 - s_2(t) \ . \tag{2}$$

(1) is very exact, however it is somewhat complex to deal with. Hence (1) is simplified by introducing the new variables as

$$r_c = \frac{R_L}{R_C+R_L}, \quad R_T(t) = s_4(t)\,R_Q + s_2(t)\,R_D, \quad x_1 = r_c\,x_1^*, \quad x_2 = r_c\,x_2^*$$

$$L = \frac{L_o}{r_c}, \quad C = \frac{C_o}{r_c}, \quad v_T(t) = s_3(t)\,V_Q + s_1(t)\,V_D \ . \tag{3}$$

Then (1) becomes

$$L\dot{x}_1 = -[R_{so} + R_T(t) + s_2(t)\, r_c R_C]\frac{x_1}{r_c} - s_1(t)\, x_2 + s_3(t)\, u^* - v_T(t) \tag{4a}$$

$$C\dot{x}_2 = s_2(t)\, x_1 - \frac{x_2}{R_L} \tag{4b}$$

$$y = s_2(t)\, R_C x_1 + x_2 \ . \tag{4c}$$

Note that no approximation is used to obtain this simplified model.

The model for the buck converter of Fig. 1b is found as

$$L\dot{x}_1 = -[R_{so} + R_T(t) + r_c R_C]\frac{x_1}{r_c} - x_2 + s_3(t)\, u^* - v_T(t) \tag{5a}$$

$$C\dot{x}_2 = x_1 - \frac{x_2}{R_L} \tag{5b}$$

$$y = R_C x_1 + x_2 \ . \tag{5c}$$

and that for the boost converter of Fig. 1c is found as

$$L\dot{x}_1 = -[R_{so} + R_T(t) + s_2(t)\, r_c R_C]\frac{x_1}{r_c} - s_1(t)\, x_2 + u^* - v_T(t) \tag{6a}$$

$$C\dot{x}_2 = s_2(t)\, x_1 - \frac{x_2}{R_L} \tag{6b}$$

$$y = s_2(t)\, R_C x_1 + x_2 \ . \tag{6c}$$

It is observed that the models for the buck and boost converters given by (5) and (6) can be deduced from the model for the buck-boost converter given by (4) if only $s_1(t)$, $s_2(t)$ and $s_3(t)$, $s_4(t)$ are set to unities, respectively. This means that it is not necessary to analyze the buck and the boost converters since they can be explained from the analysis result of the general buck-boost converter.

Then the state equation and the output equation of the buck-boost converter are obtained from (4) as

$$\begin{bmatrix}\dot{x}_1\\ \dot{x}_2\end{bmatrix} = \begin{bmatrix} -\dfrac{R_s(t)}{L} & -\dfrac{s_1(t)}{L} \\ \dfrac{s_2(t)}{C} & -\dfrac{1}{CR_L}\end{bmatrix}\begin{bmatrix}x_1\\ x_2\end{bmatrix} + \begin{bmatrix}\dfrac{1}{L}\\ 0\end{bmatrix} v_s(t) \tag{7a}$$

$$y = [\, s_2(t)\, R_C \quad 1\,]\begin{bmatrix}x_1\\ x_2\end{bmatrix} \tag{7b}$$

where

$$R_s(t) = [R_{so} + R_T(t) + s_2(t)\, r_c R_C]/r_c \ , \quad v_s(t) = s_3(t)\, u^* - v_T(t) \tag{8}$$

(7) is of the form

$$\dot{x} = A(t)x + B^* v_s(t) \tag{9a}$$

$$y = C(t)x \ . \tag{9b}$$

B. State - Space Averaging and Perturbation

The generalized state-space averaging of Part I is taken for the time-varying matrices and the source.

$$\dot{x} = \overline{A}\, x + \overline{B^*}\, v_s \tag{10a}$$

$$= \overline{\Lambda}\, x + \overline{B}\, u \tag{10b}$$

$$y = \overline{C}\, x \tag{10c}$$

where

$$\overline{\Lambda} = \begin{bmatrix} -\dfrac{R_s}{L} & -\dfrac{s_1}{L} \\ \dfrac{s_2}{C} & -\dfrac{1}{CR_L}\end{bmatrix}, \quad \overline{B^*} = \begin{bmatrix}\dfrac{1}{L}\\ 0\end{bmatrix}, \quad \overline{B} = \begin{bmatrix}\dfrac{s_3}{L}\\ 0\end{bmatrix}, \quad \overline{C} = [\, s_2 R_C \ 1\,] \tag{11}$$

and,

$$R_s = \overline{R_s(t)} = [R_{so} + R_T + s_2 r_c R_C]/r_c \ , \quad v_s = \overline{v_s(t)} = s_3 u^* - V_T = s_3 u \ , R_T = \overline{R_T(t)} = s_4 R_Q + s_2 R_D \ , V_T = s_3 V_Q + s_1 V_D \ , u = u^* - \frac{V_T}{s_3} \ . \tag{12}$$

It is found that (10b) is just the state-space averaged equation of the circuit of Fig. 2 which is the same circuit analyzed in Part I. All parasitics except the switching times are apparently disappeared in the simplified circuit. All parasitic resistances are unified into an equivalent resistor R_s and all parasitic voltage sources are integrated into an equivalent voltage source u. Thus the analyses results of Part I can be used here, considering the slight modification of the matrix C and assuming that the variations of R_s and V_T are negligible.

Hence the dc and ac parts of the perturbed equation are

$$\dot{X}_0 = A_0 X_0 + B_0 U_0$$
$$Y_0 = C_0 X_0 \tag{13}$$

and

$$\dot{\hat{x}} = (A_0 + A_2 X_0 W + B_2 U_0 W)\hat{x} + (A_1 X_0 + B_1 U_0)\hat{h}$$
$$\hat{y} = C_0 \hat{x} + C_1 X_0 \hat{h} \ . \tag{14}$$

And the operating point Y_0 and the ac transfer function $G(s)$ are

$$Y_0 = -C_0 A_0^{-1} B_0 U_0 \tag{15a}$$

$$G(s) = \frac{\hat{Y}(s)}{\hat{H}(s)} = C_0(sI - A_0 - A_2 X_0 W - B_2 U_0 W)^{-1}(A_1 X_0 + B_1 U_0) + C_1 X_0 \tag{15b}$$

where the perturbed matrices are

$$A_0 = \begin{bmatrix} -\dfrac{R_s}{L} & -\dfrac{s_1}{L} \\ \dfrac{s_2}{C} & -\dfrac{1}{CR_L}\end{bmatrix}, A_1 = \begin{bmatrix} 0 & \dfrac{1}{L} \\ -\dfrac{1}{C} & 0\end{bmatrix}, A_2 = \begin{bmatrix} 0 & -\dfrac{f\, dt_1}{L\, dx_1} \\ \dfrac{f\, dt_2}{C\, dx_1} & 0\end{bmatrix}$$

$$B_0 = \begin{bmatrix}\dfrac{s_3}{L}\\ 0\end{bmatrix}, B_1 = \begin{bmatrix}\dfrac{1}{L}\\ 0\end{bmatrix}, B_2 = \begin{bmatrix} -\dfrac{dt_1}{dx_1}\dfrac{f}{L} \\ 0\end{bmatrix}, C_0^T = \begin{bmatrix}s_2 R_C \\ 1\end{bmatrix}, C_1^T = \begin{bmatrix}-R_C \\ 0\end{bmatrix}$$

C_1 is added due to the parasitic resistance R_C. (16)

C. Pole Frequency

The poles are found by evaluating the characteristic equation

$$|sI - A_0 - A_2 X_0 W - B_2 U_0 W| = 0 \ . \tag{17}$$

The normalized natural frequency ω_n^* and normalized damping factor ζ^* are the same as those of Part I since (17) has not C_1:

$$\omega_n^* = \sqrt{\frac{r_s^* + s_1 s_2^*}{r_s^* + 1}} \ , \quad \zeta^* = \frac{1}{\omega_n^*} \ , \quad r_s^* = \frac{R_s^*}{R_L} \tag{18}$$

The switching time modulation effect is counted in r_s^* and s_2^*, and the duty cycle variation effect is represented in s_1 and s_2^*.

D. DC Gain

The dc voltage gain G_s is obtained from (15a) as

$$G_s = \frac{Y_0}{U_0} = -C_0 A_0^{-1} B_0 = \frac{1}{r_c}\frac{s_2 s_3}{r_s + s_1 s_2} \ , \quad r_s = \frac{R_s}{R_L} \tag{19}$$

G_s is slightly modified by r_c compared with the result in Part I. (19) is not the true dc voltage gain, however, since U_0 is

not the true source voltage U_0^*. From (12) the ratio of U_0 to U_0^* is determined as

$$G_c = \frac{U_0}{U_0^*} = 1 - \frac{V_T}{s_3 U_0^*} . \quad (20)$$

Then the true voltage gain G_v is evaluated as

$$G_v = \frac{Y_0}{U_0^*} = \frac{Y_0}{U_0}\frac{U_0}{U_0^*} = G_s G_c = \frac{1}{r_c}\frac{s_2 s_3}{r_s + s_1 s_2}\left[1 - \frac{V_T}{s_3 U_0^*}\right] \quad (21)$$

It is notable that the G_s and G_c are concerned with the switching loss and conduction loss respectively.

E. Efficiency

The current gain G_i which is the ratio of the output current I_o to the input current I_i is obtained as

$$G_i = \frac{I_o}{I_i} = \frac{s_2 X_1}{s_4 X_1} = \frac{s_2}{s_4} \quad (22)$$

Then the efficiency η becomes

$$\eta = \frac{Y_0 I_o}{U_0^* I_i} = G_v \cdot G_i = \frac{1}{r_c}\frac{s_2^2 s_3}{(r_s + s_1 s_2)s_4}\left[1 - \frac{V_T}{s_3 U_0^*}\right] = \eta_s \cdot \eta_c \quad (23)$$

where η_s and η_c are the efficiency degenerations due to where η_s and η_c are the efficiency degenerations due to switching loss including parasitic resistances and conduction loss, respectively. They are given as

$$\eta_s = \frac{1}{r_c}\frac{s_2^2 s_3}{(r_s + s_1 s_2)s_4}, \quad \eta_c = 1 - \frac{V_T}{s_3 U_0^*} . \quad (24)$$

The η_c is much deteriorated when the source voltage is low and the duty cycle (for the buck and buck-boost converters only) is low. For example, the efficiency becomes not more than 70 percents when $V_T = V_Q = V_D = 0.6$ volt, the source voltage is 10 volt and the duty cycle is 0.2 even though the switching frequency is low. Hence it is desirable to set the duty cycle near to unity for the buck converter to avoid excessive conduction loss.

In the low voltage high efficiency applications, η_c may be a reference for determining η_s or accordingly the switching frequency. If η_s is much less than η_c then the switching frequency becomes unacceptably too low, which results in very large filter size. A good example is to let η_s be the same as η_c.

III. EXPERIMENT

The boost converter shown in Fig. 3 is selected to verify the analytical results. The ratings of the switching devices are selected high enough to overcome sevear experiment conditions. Since several switching times are very sensitive to the base driver, temperature and current, the base driver is simplified and the switching times are measured case by case at the ambient temperature of 25 degree C. Fig. 4 is the picture of a practical switching case. The upper is the base drive voltage, the middle is the collector-emitter voltage of the transistor and the lower is the diode current. The parameters of the switching devices are

Tr : 600 volt, 200 ampere, $V_Q = 0.7$ volt, $R_Q = 0.035$ ohm

Diode : 600 volt, 200 ampere, $V_D = 0.7$ volt, $R_D = 0.25$ ohm (25)

The natural frequency of the open loop system is determined by inserting a small step change in the duty cycle and measuring the rise time and the overshoot of the response. It is depicted in Fig. 5. It is observed that the parasitic effects become dominant as the switching frequency increases. Unfortunately the data is not based on the uniform temperature distribution due to the difficulty in keeping the temperature of the switches be constant.

The voltage gain is measured by dividing the output voltage by the input voltage for the wide range of duty cycle. That is shown in Fig. 6 for several switching frequencies with a large deviation from the ideal switching case. It is observed that the switching loss is the major source of the degeneration of the voltage gain.

The efficiency is calculated by measuring the currents and the voltages of the input and output, and comparing the input and output powers. It is shown in Fig. 7 for several duty cycles. The tendency is somewhat different from the constant switching time case of Part I. The difference is due to the variation of the switching times by the temperature. A good way to determine the efficiency in the practical switching case is to set the operating temperature first and then measure the switching times at the temperature. This may be one of the practical way to determine the switching frequency for a given efficiency.

In a whole the deviations from the ideal converter due to the parasitics (especially finite switching times) are not negligible and thus they should be counted in the design of the high performance converters.

IV. SUMMARY

The analytical results are tabulated in Table using the normalized resistance r_s, r_c, the conduction voltage V_T and the average switching functions s_1, s_2, s_3 and s_4. The results are simple and exact in spite of several parasitics. The pole frequency, dc voltage gain, dc current gain and efficiency of the buck and boost converters are those of the buck-boost converter whose s_1, s_2 and s_3, s_4 are set to 1's, respectively.

The dc voltage gain and efficiency are also found to be just the products of those of the conduction loss term and those of the switching loss term.

V. CONCLUSION

All parasitics such as switch conduction voltages, conduction resistances, switching times and ESR's of capacitors are counted in the new state-space modeling which is based on non-ideal switching functions. The results are, however, not complex and are verified by the experiment. Hence it is believed that this modeling is both simple and exact, which is crucial for the application of the modeling to the industry. The results of the conventional modelings with parasitics are improved a little and integrated by this modeling. So this may be a good summary of the parasitics. An interesting result is that a very simple equivalent circuit can be deduced from the complex original circuit that has all parasitics. The parasitic effects become dominant as the switching frequency, parasitic resistances, duty cycle (for the boost converter case) and conduction voltage increase and the duty cycle (for the buck converter case) and source voltage decrease. Those of the buck-boost converter become dominant as the duty cycle approaches to either zero or unity.

This modeling may be extended to other converters such as resonant converters and inverters to find the exact voltage and current gains and efficiencies.

REFERENCES

[1] W. M. Polivka, P. R. K. Chetty and R. D. Middlebrook," State-space average modeling of converters with parasitics and storage-time modulation," in IEEE Power Electronics Specialists Conf. Rec., pp. 219- 243, 1980.

[2] R. C. Wong, G. E. Rodriguez, H. A. Owen, Jr. and T. G. Wilson," Application of small signal modeling and measurement techniques to the stability analysis of an integrated switching-mode power system," in IEEE Power Electronics Specialists Conf. Rec., pp. 104-118, 1980.

[3] G. Eggers," Fast switches in linear networks," IEEE Trans. Power Electronics, vol. PE-1, No. 3, pp. 129-140, July 1986.

[4] R. D. Middlebrook and Slobodan Cuk," Modeling and analysis methods for DC-to-DC switching converters," invited review paper, IEEE International Semiconductor Power Converter Conf. 1977 Rec., pp. 90-111.
[5] C. T. Rim, G. B. Joung and G. H. Cho , " A state space modeling of non-ideal DC-DC converters," in IEEE Power Electronics Specialists Conf. Rec., pp. 943-950, 1988.

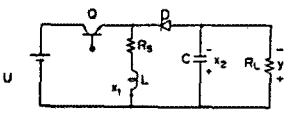

Fig. 2 The equivalent simplified buck-boost converter.

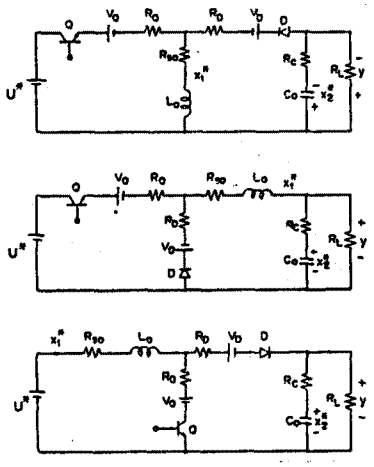

Q,D : switches with finite switching times

Fig. 1 Original circuits with all parasitics.

(a) buck-boost converter

(b) buck converter

(c) boost converter

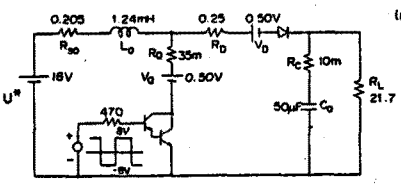

Fig. 3 The experimental boost converter.

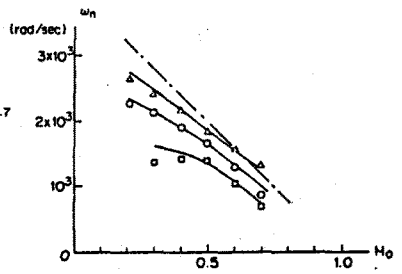

Fig. 5 The natural frequencies of the experimental boost converter.

——— : theory, - - - : ideal case, △ : f= 5 k Hz,

○ : f= 10 k Hz, □ : f= 20 k Hz

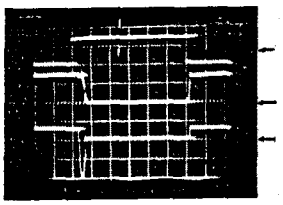

Fig. 4 The switching waveforms.

(the upper : base drive input voltage; 10 volt / div. ; 10 μ s / div.

the middle : collector-emitter voltage; 20 volt / div. ,

the lower : diode current; 5 ampere / div. , ——— : GND)

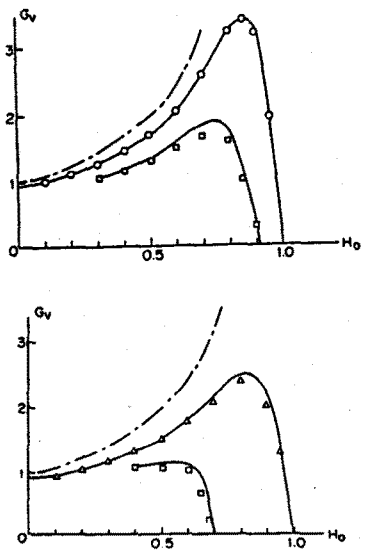

Fig. 6 The voltage gains of the experimental boost converter.

(a) ——— : theory, - - - : ideal case, ○ : f=1 k Hz, □ : f= 20 k Hz

(b) ——— : theory, - - - : ideal case, △ : f=5 k Hz, □ : f= 50 k Hz

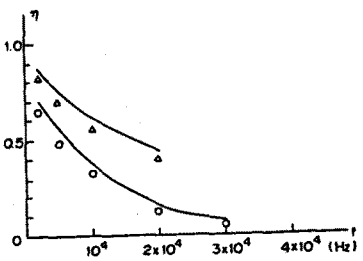

Fig. 7 The efficiencies of the experimental boost converter.

——— : theory, △ : H_0= 0.3, ○ : H_0= 0.7

type	Buck	Boost	Buck-boost
items	F_1	F_2	F_3
ω_n^*	1	$\sqrt{\frac{r_s^* + s_1 s_2^*}{r_s^* + 1}}$	$\sqrt{\frac{r_s^* + s_1 s_2^*}{r_s^* + 1}}$
ζ^*	1	$\frac{r_s^* + 1}{\sqrt{r_s^* + s_1 s_2^*}}$	$\frac{r_s^* + 1}{\sqrt{r_s^* + s_1 s_2^*}}$
G_s	$\frac{1}{r_c}\frac{s_3}{r_s + 1}$	$\frac{1}{r_c}\frac{s_2}{r_s + s_1 s_2}$	$\frac{1}{r_c}\frac{s_2 s_3}{r_s + s_1 s_2}$
G_d	$1 - \frac{V_T}{s_3 U^*}$	$1 - \frac{V_T}{U^*}$	$1 - \frac{V_T}{s_3 U^*}$
G_i	$\frac{1}{s_4}$	s_2	$\frac{s_2}{s_4}$
G_v	$G_s \cdot G_c$		
η_s	$G_s \cdot G_i$		
η_c	G_c		
η	$\eta_s \cdot \eta_c = G_s \cdot G_c \cdot G_i$		
$F_1 = F_3\|_{s_1 \to s_2 = 1}$		$F_2 = F_3\|_{s_3 \to s_4 = 1}$	
$r_s = R_s/R_L$, $r_s^* = R_s^*/R_L$, $r_c = \frac{R_L}{R_C + R_L}$			
$R_s = (R_{s0} + R_T + s_2 r_c R_C)/r_c$, R_s^* :see Part 1			

Table Summaries of parasitic effects.